

# Generation of optical combs in a whispering gallery mode resonator from a bichromatic pump

Dmitry V. Strekalov and Nan Yu

*Jet Propulsion Laboratory, California Institute of Technology,  
4800 Oak Grove Drive, Pasadena, California 91109-8099*

(Dated: February 26, 2019)

We report an experimental realization of an optical comb arising from a whispering gallery mode resonator pumped by two optical frequencies. Two externally excited resonator modes couple due to Kerr nonlinearity to initially empty modes and give rise to new frequency components. This process is much more efficient than the previously reported single-pump four-wave mixing. As a result, only a few milliwatt pump is required to generate strong secondary fields. In further contrast with the single-pump approach, this process is thresholdless, so the secondary frequency components can efficiently generate those of higher orders and so on, in a cascade process leading to an optical comb.

PACS numbers: 42.60.Da, 42.65.Ky, 42.65.Hw

Optical frequency combs [1, 2] have found their applications as optical clocks and frequency standards of extremely high accuracy [3], including those for astronomy [4] and molecular spectroscopy [5, 6]. They have also been proposed for use in quantum information processing [7, 8]. One method to generate optical combs is via four-wave mixing in a resonator with Raman or Kerr nonlinearity [9, 10, 11, 12, 13]. In this case the comb arises from direct or cascaded frequency conversion processes, which requires very high effective nonlinearities. The latter can be achieved by using the whispering gallery mode (WGM) resonators, known for their extremely high  $Q$  factors, reaching  $5 \times 10^{10}$  in crystalline materials [14].

In monochromatically pumped Kerr-based optical comb sources two pump photons are converted into a quantum-correlated photon pair. The energy diagram of this process is shown in Fig. 1(a). This process populates the adjacent to the pump pair of modes as well as those two, three, etc., of the resonator free spectral ranges (FSR)  $\Omega$  away from the pump. The comb range is limited by the resonator dispersion, which makes excitation of distant pairs of modes incompatible with the energy conservation. To generate such a comb in a WGM resonator, the pump has to exceed a certain threshold power  $P_{th}$ , inversely proportional to the  $Q^2$  [15].

We realized a different configuration of a four-wave mixing comb using two pumps coupled to two WGMs one or several FSRs apart. Then instead of coupling two vacuum and two (degenerate) pump fields, the leading-order interaction couples three pump fields and one vacuum field. For example, on the energy diagram in Fig. 1(b) two pump photons with frequency  $\omega_1$  are absorbed, and one pump photon with frequency  $\omega_2 > \omega_1$  is emitted, along with the photon with  $\omega_- = 2\omega_1 - \omega_2$ . A symmetric process will lead to generation of a photon with  $\omega_+ = 2\omega_2 - \omega_1$ . Since the pump field is usually much stronger than the new fields, the non-degenerate four-wave mixing is expected to be much more efficient than the degenerate. Furthermore, as we will see below, the non-degenerate process is thresholdless. It occurs at any pump power, which allows one to avoid the undesirable

high-power effects such as thermorefractive oscillations [15] and stimulated Raman scattering. The high efficiency and absence of the threshold in the studied process leads us to expect that the newly generated frequency components will efficiently generate further components, spreading into a comb.

Our experimental setup diagram is shown in Fig. 1(c). We used a fluorite resonator with 13.56 GHz FSR. Fluorite has nearly linear dispersion at the wavelength of 1.5 micron, so the resonator spectrum around this wavelength is highly equidistant. Light was coupled in and out of the resonator using two optical fibers polished at the optimal coupling angle [16]. The light from the input fiber reflected from the resonator's rim was collected by a photo detector to observe the spectrum of the resonator.

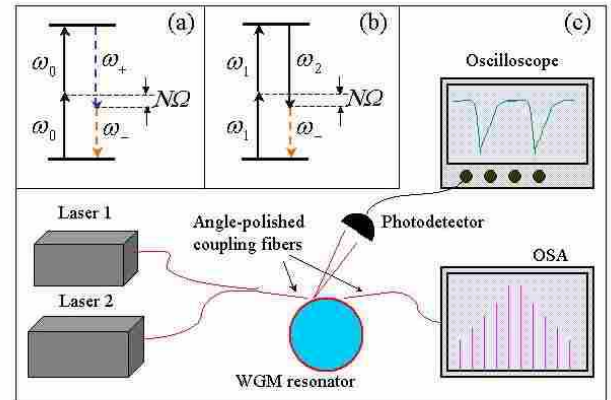


FIG. 1: Energy diagrams of previously (a) and presently realized (b) four-wave mixing processes generating a frequency comb. The experimental setup (c).

The input fiber combined light from two lasers centered at 1560 nm. Both laser's frequencies were simultaneously scanned around the selected WGMs of the same family. This was achieved by fine-tuning each frequency until the selected resonances observed by the photo detector overlap. The resonator quality factor  $Q = 10^8$  was made relatively low to increase the linewidth and to make the

overlap easier to achieve. The optical spectrum analyzer (OSA) connected to the output fiber was continuously acquiring data. The OSA was set to retain the peak power values, therefore a trace recorded for a sufficiently long period of time represented the situation when both lasers are fully coupled to the WGMs.

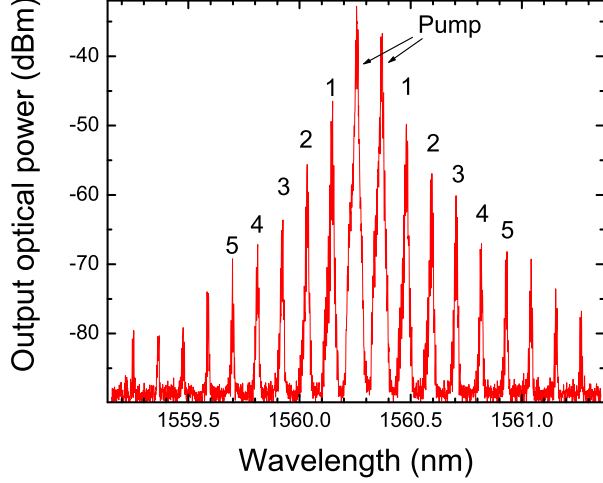


FIG. 2: A typical spectrum of a bichromatically-pumped fluoro WGM resonator. The two highest peaks correspond to the two pumps, each of 2.9 mW at the input.

A typical comb generated by two pumps of  $P_1 = P_2 = 2.9$  mW set one FSR apart is shown in Fig. 2. The pump output power is considerably lower than the input mainly because of weak output coupling (so as not to overload the resonator), but also because of linear and nonlinear loss. We did not see any threshold pump power required for the onset of the nonlinear oscillations. This measurement was repeated with the lasers set two, three and ten FSRs apart. We had to stop at the ten FSR separations, because the lasers could not be tuned further. No significant difference between these measurements and the first one was observed. A comb spectrum corresponding to the ten FSR separation and the pump power  $P_1 = P_2 = 4.75$  mW is shown in Fig. 3.

Our experiment can be described within the general theoretical model of Kerr-coupling of the WGMs [15]. The difference in the present treatment is that the partial degeneracy of the Hamiltonian in [15] is removed, and the leading-order process is a four-mode interaction rather than three-mode. The Hamiltonian  $H = H_0 + V$  describing our system includes the following terms:

$$\begin{aligned} H_0 &= \hbar\omega_a a^\dagger a + \hbar\omega_b b^\dagger b + \hbar\omega_c c^\dagger c + \hbar\omega_d d^\dagger d, \\ V &= -\hbar\frac{g}{2} : (a + b + c + d + h.c.)^4 :, \end{aligned} \quad (1)$$

where  $c$ ,  $a$ ,  $b$ , and  $d$  are photon annihilation operators at frequencies  $\omega_c < \omega_a < \omega_b < \omega_d$ , respectively. The

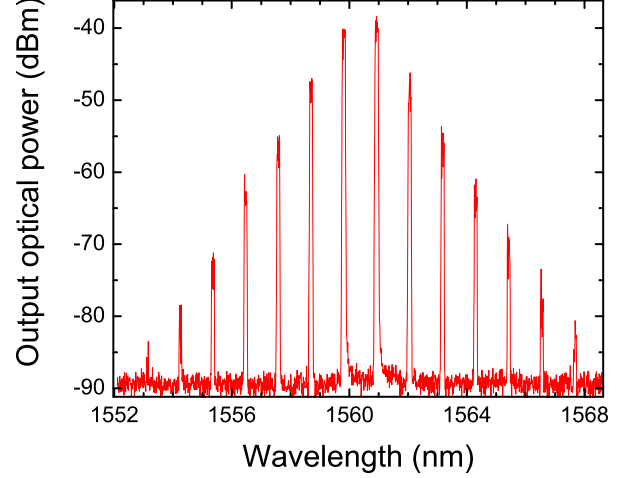


FIG. 3: The spectrum for  $P_1 = P_2 = 4.75$  mW and 10 FSR (135.6 GHz) pump separation.

coupling constant  $g$  is found in [15]:

$$g = \omega \frac{n_2 \hbar \omega c}{n_0 \mathcal{V} n_0}, \quad (2)$$

where  $n_2$  is the Kerr nonlinearity of the resonator material,  $n_0$  is its refraction index and  $\mathcal{V}$  is the mode volume.

Notice that the fields represented by the operators  $a$  and  $b$  are strong pump fields, while the fields represented by  $c$  and  $d$  are initially vacuum fields. In Hamiltonian (1) we will only retain the leading terms with at least three pump fields operators. The equations of motion then take on the following form:

$$\begin{aligned} \dot{a} &= -i\omega_a a + 6ig(a^\dagger aa + 2ab^\dagger b + 2a^\dagger bc + bbd^\dagger), \\ \dot{b} &= -i\omega_b b + 6ig(b^\dagger bb + 2ba^\dagger a + 2b^\dagger ad + aac^\dagger), \\ \dot{c} &= -i\omega_c c + 6igaab^\dagger, \\ \dot{d} &= -i\omega_d d + 6igbba^\dagger. \end{aligned} \quad (3)$$

Following the steps of [15] we introduce the Langevin forces and write the system (3) in the stationary state as

$$\begin{aligned} \gamma a &= 6ig(a^\dagger aa + 2ab^\dagger b + 2a^\dagger bc + bbd^\dagger) + f_a, \\ \gamma b &= 6ig(b^\dagger bb + 2ba^\dagger a + 2b^\dagger ad + aac^\dagger) + f_b, \\ \gamma c &= 6igaab^\dagger + f_c, \\ \gamma d &= 6igbba^\dagger + f_d, \end{aligned} \quad (4)$$

where the loss rate  $\gamma$  and optical frequency  $\omega$  are assumed to be the same for all modes, and

$$\langle f_{a,b} \rangle = \sqrt{\frac{2\gamma P_{a,b}}{\hbar\omega}}, \quad \langle f_{c,d} \rangle = 0. \quad (5)$$

Let us neglect the self- and cross-phase modulation terms in the first two equations (4). Then we find

$$\langle a \rangle = \sqrt{\frac{2P_a}{\gamma\hbar\omega}}, \quad \langle b \rangle = \sqrt{\frac{2P_b}{\gamma\hbar\omega}}, \quad (6)$$

$$\langle c \rangle = \frac{6gP_a\sqrt{P_b}}{\gamma} \left( \frac{2}{\gamma\hbar\omega} \right)^{3/2}, \quad (7)$$

$$\langle d \rangle = \frac{6gP_b\sqrt{P_a}}{\gamma} \left( \frac{2}{\gamma\hbar\omega} \right)^{3/2}. \quad (8)$$

Using Eq. (6) as the connection between the internal field and external power coupled in and out of the resonator (assuming critical coupling), we finally arrive at

$$P_c = P_b \left( \frac{P_a}{P_{sat}} \right)^2, \quad P_d = P_a \left( \frac{P_b}{P_{sat}} \right)^2, \quad (9)$$

$$P_{sat} \equiv \frac{\gamma^2\hbar\omega}{12g} = \frac{2\pi\mathcal{V}}{3n_2\lambda} \left( \frac{n_0}{4Q} \right)^2 \approx \frac{1}{18}P_{th}, \quad (10)$$

where  $P_{th}$  is the threshold power for the single-pump hyperparametric oscillations, introduced in [15]. Assuming  $\lambda = 1.56 \mu\text{m}$ ,  $n_0 = 1.44$ ,  $n_2 = 3.2 \cdot 10^{-16} \text{ cm}^2/\text{W}$ ,  $Q \approx 10^8$ ,  $\mathcal{V} \approx 10^{-4} \text{ cm}^3$ , we find for our resonator  $P_{sat} \approx 50 \text{ mW}$ . This value is only the order-of-magnitude estimate because the actual shape of our hand-polished resonator is unknown, and the mode volume  $\mathcal{V}$  cannot be estimated better than to the order of magnitude.

To compare the result (9) with the experimental data we need to take into account the unknown output coupling efficiency. This factor can be eliminated if we plot the output power normalized to the average  $(P_c(P) + P_d(P))/2$  which is evaluated at a low pump power  $P = P_a = P_b$ , e.g.  $P = 0.75 \text{ mW}$ . This plot is shown in Fig. 4 on a log-log scale, jointly for the experiments with one, two, three and ten FSRs of the pumps separation. The slope of the linear fit of this plot gives the power dependence of  $P_{c,d}(P)$ , and should be equal to three according to Eq. (9). However from the fit in Fig. 4 we find  $P_{c,d}(P) \propto P^{2.13 \pm 0.16}$ . While because of the pump depletion the expected power dependence could be slower than the predicted cubic, it is puzzling that it was found to be almost exactly quadratic.

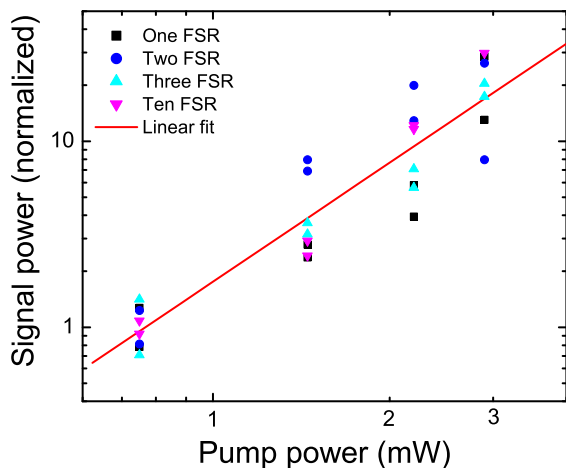


FIG. 4: Normalized power of the first-order frequency components vs. the pump power: the data and the fitting curve.

We have already mentioned that the studied process is thresholdless. As a consequence, it can be efficiently cascaded, with each excited mode playing the role of a new pump. A rigorous analysis of such a nonlinear cascade dynamics is difficult. Here we describe a simplified model based on Eq. (9), which takes into account only the leading-order conversion channels and neglects depletion of the modes serving as the pumps. The diagrams of such channels generating the blue-shifted first- through sixth-order comb components are shown in Fig. 5. Similar diagrams can be drawn for the red-shifted components. In Fig. 5, every pair of arrows point from a mode in which a pair of photons is annihilated to the modes in which the photons are created. It is easy to see from (9) that the powers of the red- and blue-shifted components of the same order  $n$  are equal and scale with the parameter  $\xi \equiv (P/P_{sat})^2$  as

$$P_c^{(n)} = P_d^{(n)} = P_n \xi^n. \quad (11)$$

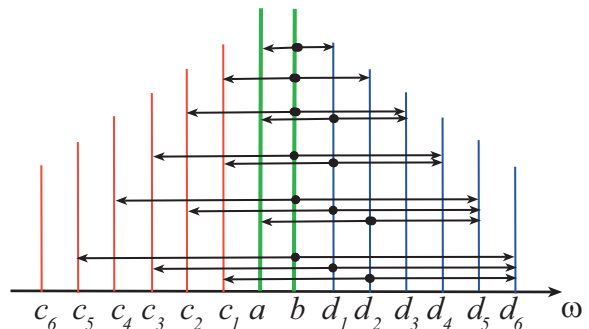


FIG. 5: The dominant channels for cascading the optical comb from a bichromatic pump.

Each channel shown in Fig. 5 annihilates a photon pair in some blue-shifted mode  $m$  and couples it to a yet unpopulated blue-shifted mode  $n > m$  and to already populated red-shifted mode  $n - 2m - 1 < n$ . According to (9) the power therefore delivered to the mode  $n$  is

$$P_{m \rightarrow n} = P_{n-2m-1} \xi^{n-2m-1} \left( \frac{P_m \xi^m}{P_{sat}} \right)^2. \quad (12)$$

In our model we disregard interference between different channels and simply add up the powers. This approximation may be suitable when the number of such channels is large. We arrive at the following recursive relation:

$$P_n = \sum_{m=0}^{(n-1)/2} (P_m/P)^2 P_{n-2m-1}, \quad (13)$$

which yields a sequence  $P_n/P = 1, 1, 2, 3, 5, 8, 16, 27, \dots$

Equations (11) and (13) allow us to approximately fit the comb envelope, see e.g. Fig. 6. The comb shown in this figure is generated by two pumps of  $4.75 \text{ mW}$  each, set three FSRs apart. Also shown are the envelope fitting function based on Eqs. (11) and (13), and

the exponential envelope which results from the analysis assuming a single excitation channel for each mode. In both cases the parameter  $\xi$  is found from the averaged ratio of the measured  $P^{(2)}$  and  $P^{(1)}$ , see Eq. (11). We see that the multi-channel model approximates the observed comb more accurately than the single-channel one.

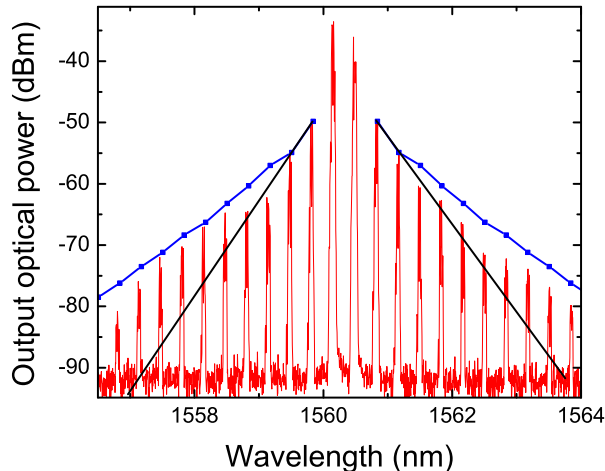


FIG. 6: A three-FSR-spaced comb generated by two 4.75 mW pumps is fit by the envelope functions based on a single-channel excitation (solid straight line) and on multiple excitations channels (dotted broken line.)

To summarize, we have demonstrated a new and highly efficient method of generating optical combs in WGM resonators with Kerr nonlinearity. Even with a relatively low- $Q$  resonator multiple new frequency components have been observed with only a few milliwatt of the external CW pump power. The theoretical prediction of the absence of the threshold pump power has been confirmed. Our analysis of the comb envelope shape, based

on the concept of the multi-channel cascade excitation, reasonably agrees with the experiment. The dependence of the comb components powers on the pump power did not agree with our theoretical model, which may be in part due to the pump depletion.

The frequency spacing of a bichromatically pumped comb is determined by the pumps detuning  $\omega_b - \omega_a$ , whose stability therefore determines stability of the entire comb. Phase-locking the lasers beat note to a high-stability reference oscillator one can have the comb stability matching that of a state-of-the-art frequency reference. The situation is different for the single-pump comb, whose frequency stability improves as  $Q^2$  [15], obeying the Schawlow-Townes formula. On the other hand, the range of the dispersion-limited comb scales as the linewidth, i.e.  $1/Q$ . An advantage of the bichromatic pump approach is therefore that it provides for superior stability even with low- $Q$  resonators that can support broader-range combs.

We demonstrated the comb spacing varying from one to ten FSR without any appreciable change in the comb behavior. This suggests that the spacing could be made even larger. Variable spacing of the comb may not be only technically convenient for the spectroscopy applications, but also may partially compensate the resonator dispersion, which is the main factor limiting the comb span. We also would like to point out an interesting possibility of creating Moire comb pattern, by using three or more unequally spaced pump frequencies. This may enable an interesting approach to optical synthesizers.

The research described in this paper was carried out by the Jet Propulsion Laboratory, California Institute of Technology, under a contract with the National Aeronautics and Space Administration. Dmitry Strekalov also thanks Drs. Andrey Matsko of OEwaves and Ivan Grudinin of Caltech for helpful discussions.

- 
- [1] T. Udem, R. Holzwarth, and T.W. Hansch, *Nature* **416**, 233-37 (2002).
  - [2] J. Ye and S.T. Cundiff, eds. *Femtosecond optical frequency comb technology*. (Springer, New York, 2005).
  - [3] L. Ma, Z. Bi, A. Bartels, L. Robertsson, M. Zucco, R. Windeler, G. Wilpers, C. Oates, L. Hollberg, and S.A. Diddams, *Science*, **303**, 1843-1845, (2004).
  - [4] Chih-Hao Li et al., *Nature* **452**, 610-612 (2008).
  - [5] M.J. Thorpe, K.D. Moll, J.J. Jones, B. Safdi, and J. Ye, *Science* **311**, 1595-99 (2006).
  - [6] S.A. Diddams, L. Hollberg, and V. Mbele, *Nature* **445**, 627630 (2007).
  - [7] H. Zaidi, N.C. Menicucci, S.T. Flammia, R. Bloomer, M. Pysher, and O. Pfister, *Las. Phys.* **18**, 659 (2008).
  - [8] N.C. Menicucci, S.T. Flammia, and O. Pfister, *ArXiv quant-ph/0804.4468* (2008).
  - [9] S.M. Spillane, T. J. Kippenberg, and K. J. Vahala, *Nature* **415**, 621 (2002).
  - [10] A. A. Savchenkov, A. B. Matsko, D. V. Strekalov, M. Mohageg, V.S. Ilchenko and L. Maleki, *Phys. Rev. Lett.* **93**, 24395 (2004).
  - [11] T. J. Kippenberg, S.M. Spillane, and K. J. Vahala, *Phys. Rev. Lett.*, **93**, 083904 (2004).
  - [12] P. DelHaye, A. Schliesser, O. Arcizet, T. Wilken, R. Holzwarth and T. J. Kippenberg, *Nature*, **450**, 1214-17 (2007).
  - [13] A.A. Savchenkov, A.B. Matsko, V.S. Ilchenko, I. Solomatine, D. Seidel, and L. Maleki, *Phys. Rev. Lett.*, **101**, 093902 (2008).
  - [14] I. Grudinin, A. Matsko, A. Savchenkov, D. Strekalov, V. Ilchenko, and L. Maleki, *Opt. Comm.*, **265**, 33-38 (2006).
  - [15] A. B. Matsko, A. A. Savchenkov, D. Strekalov, V. S. Ilchenko and L. Maleki, *Phys. Rev. A* **71**, 033804 (2005).
  - [16] V. S. Ilchenko, X. S. Yao, and L. Maleki, *Opt. Lett.* **24**, 723-725 (1999).